Influence of Changing Location of the Equilateral Triangle Cylinder on Characteristics of Fluid Flow and Forced Convection Heat Transfer: A Numerical Study

Sarmad A. Ali

Department of Automobile Engineering, College of Engineering-Al Musayab, University of Babylon, Province of Babylon,
Email: sarmad.ahmed96@uobabylon.edu.iq
https://orcid.org/0009-0001-9231-9523

Abstract

A numerical investigation has been conducted on heat transport in a domain when an equilateral triangular cylinder of (15 mm) is present. A flow analysis is conducted using a Reynolds number (Re) ranging from 100 to 500 on a cylinder encircling a laminar regime. The flowing medium, air, is thought to have a constant Prandtl number. A two-dimensional method is used to simplify the problem. The governing equations are solved using momentum, energy, and continuity equations. Studying the effect of changing the position of the cylinder within the computational domain on several parameters such as temperature distribution, pressure, velocity, streamline, surface temperatures, Nusselt number (Nu), friction factor, and the drag and lift coefficient (C_D and C_L). The results of the current study showed that the location of the cylinder affects the characteristics of airflow, where the first location gave the best improvement of heat transfer compared to other locations; also, the surface temperature gradually decreases by increasing the Reynolds number and increases by changing the location towards the axis of fluid flow and the friction factor decreased significantly by increasing the air velocity around the cylinder. The percentage difference of the temperature distribution rate of the surface for a computational domain of the cylinder locations (2, 3 and 4) compared to the first location (48.00, 49.00, and 46.00 %), respectively.

Keywords- Equilateral Triangle Cylinder, Friction Factor, Laminar Flow, Heat Transfer, Location.

1. INTRODUCTION

Due to the scientific importance of thermal engineering and fluid mechanics and the theoretical and practical in the field of engineering, the flow has been extensively studied around trickling cylinders. The characteristics of the external flow are different from those of the internal one, where the external fluid flow is above the surface, while the internal flow is in the channel. In civil, mechanical, and other fields, cylindrical-circular structures are used in various devices. A system is found in the cooling system of nuclear power plants, buildings, chimneys, offshore structures, and structures resembling cylinders, both alone and in a set in the design of heat exchangers. Air and water were used as a flowing medium in power lines, grids, screens, and cables. Many important physical phenomena determine and manifest the flow around cylinders, including vortex shedding, flow separation, and transforming laminar flow into turbulence. Zoubair Boulahia et al. [1] presented a numerical study to investigate the flow of a mixed convection type of a circular cooling obstacle in a square cavity. Using a simple algorithm of the finite volume estimation method, the governing equations of the fluid flow were solved, including the Navier-Stokes two-dimensional equation, continuity, and energy balance. The effect of the outlet-outlet location on the volume fraction of nanoparticles and the Richardson number have been studied. The outlet port was varied from top to bottom to achieve the maximum heat transfer rate. Ram Ranjan et al. **[2-6]** displayed a numerical study of forced convection to investigate the properties of flow and two-dimensional heat transfer around a cylinder within a computational domain. Solving the flow equations using commercial code and different Reynolds number ranges and using techniques that improve and enhance the heat transfer process, such as porous media and nanofluids. Hao Ma and Zhipeng Duan [7] systematically studied heat transfer and fluid flow around a circular cylinder to determine the concept of drag coefficient by introducing a new drag coefficient representative. It was proved that the new modified drag coefficient is a dimensionless parameter for describing the fluid; this is to describe the fluid more suitable for the flow of physical behavior. As a result of the disturbance in predicting the behavior of heat and mass transfer, the symmetry breaking of the global structure of the flow field increases. Elham Maghsoudi [8] presented a numerical study to investigate the properties of gas and heat transfer by the laminar flow of a circular cylinder. The limits of sliding and temperature jumping were applied to the cylinder wall. As a result of the difference in the Reynolds and Knudsen numbers, changes in the sliding speed and heat transfer at the cylinder wall were calculated. Due to the sliding condition an increase in speed is observed at the wall with an increase in the number of Knudsen. K. Vajravelu, et al. [9] researched a numerical study of the analysis

of the effects of thermophysical properties of a viscous liquid produced by a cylinder in the presence of internal thermogenesis and with asymmetric flow. It was assumed that the cylinder is extended in the axial direction, the surface temperature is linearly different, and the speed is linear. The partial differential equations governing the flow have been transformed into nonlinear Ordinary Differential Equations combined with variable coefficients. The equations governing the physical phenomenon showed that the properties of heat transfer and fluid flow depend on several parameters, including the viscosity of the liquid, bending, injection/suction, thermal conductivity, and Prandtl number. Ghassan Smaisim et al. [10] researched a numerical (ANSYS fluent) and experimental study of forced convection heat transfer in a horizontal cylinder in two conditions, the first stationary and the second rotary, for the Reynolds number range (160-960) and rotational speed for ranges (0-6). The cylinder's surface temperatures were measured using a thermal camera, and the flow profile was acquired using photography. The results showed that at the same Reynolds number, the upper limit of the average heat transfer occurs, while at the maximum Reynolds rotational number, the minimum value occurs. Ram Prakash Bharti et al. [11] displayed a finite volume technique built on a Cartesian grid system has been used to study forced convection heat transfer from an unconfined circular cylinder in the steady cross-flow regime in the range of Re of (10-45) and Pr of (0.7 - 400). The numerical findings are utilized to create basic correlations for the Nusselt number as a function of the relevant dimensionless variables. The effects of Re, Pr, and thermal boundary conditions for the average Nusselt number have also been studied to provide more physical insight into the nature of the flow. These effects can be seen in the temperature field close to the cylinder and the local Nusselt number distributions. Suvanjan Bhattacharyya et al. [12] presented a numerical investigation that has been conducted on heat transport in a channel with a hexagonal cylinder present. A hexagonal cylinder surrounded by a laminar and turbulent regime is subjected to a flow study at turbulence intensities of 5% to 50% and Reynolds numbers ranging from 100 to 50,000. Since air is a flowing medium, its Prandtl number is thought to remain constant. Three dimensions are used to simplify the problem. The governing equations are solved using continuity, momentum, and energy equations. Calculations of stable versions are performed using the Transition SST Model. Correlations are used to validate the analytic results, and it is found that the results are comparable to one another. Gurminder Singh and Oluwole Daniel Makinde [13] presented an analysis using numerical methods is conducted to examine the heat transfer in the axisymmetric boundary layer flow of a viscous incompressible fluid in the axial direction of a vertical stationary isothermal cylinder when there is a uniform free stream with momentum slip. The continuity, momentum, and energy equations that control the flow are converted into non-similar boundary layer equations and numerically solved using the asymptotic series approach and Shanks transformation. The shooting technique and the Runge-Kutta fourth order system are both part of the numerical scheme. In addition to analyzing the flow for both opposing and aiding buoyancy, a graphic representation of the effects of various factors on the fluid velocity, temperature distribution, heat transfer, and shear stress parameters is provided. A. H. Majeed et al. [14] displayed a numerical study involves a thorough examination of the hydrodynamic forces under magnetohydrodynamics and the forced convection thermal flow across a heated cylinder with insulated plates positioned at the walls. Within the transverse direction of flow, the magnetic field is applied. The Galerkin finite element scheme has been applied to the two-dimensional nonlinear partial differential equations system. A crude hybrid computational grid is created and refined further to provide the exact result. The best cases are chosen using average Nusselt numbers, drag and lift coefficients, pressure drop decrease versus cylinder thickness ratios, and flow patterns. H. S. Yoon et al. [15] examined heat transfer and two-dimensional laminar fluid flow via a circular cylinder close to a moving wall numerically. Numerical simulations are conducted for a circular cylinder at various Reynolds numbers, namely 100, 140, and 180, to thoroughly analyze how a moving wall alters the flow and thermal fields surrounding the cylinder. The result shows that the vortex shedding those forms in the wake is reduced, and the lift coefficient's fluctuating amplitude decreases as the gap ratio drops. Consequently, as a function of the gap ratio and the Reynolds number, the drag, lift coefficients, and Nusselt number that characterize the fluid flow and heat transfer properties also change.

The current study seeks to investigate the effect of changing the positions of a cylinder with an equilateral triangular cross-section of (15mm) on the characteristics of airflow and heat transfer by forced convection with laminar flow through the study of several parameters, including the drag and lift coefficient, friction factor, surface temperature and the Nusselt number in different ranges of the Reynolds number of (100 -500). The surface of the cylinder is exposed to a constant heat flux of (10000 W/m^2), while the walls of the computational domain (L=120 mm and W=50 mm) are thermally insulated.

2. METHODOLOGY

Transferring heat by forced convection and the movement of liquids by laminar flow around a cylinder with an equilateral triangular cross-section and at different locations is a difficult and complex procedure. As a result, the efficiency of contract simulation is affected by the thermal differences of various transactions. Several elements affect the success of the numerical simulation process, including the mesh generation, the creation of geometric models, and the appropriate choice of numerical computing technology.

3. NUMERICAL METHOD

3.1 Technique of Simulation

In the current work, the airflow around an equilateral triangular cylinder of 15 mm has been modeled at various positions using a 2-dimensional model design. The current design was modeled using ANSYS Fluent 23.0 to evaluate the flow and heat transfer characteristics. The computational domain in Figure (1) was constructed using a design modeler. Its dimensions are 120 mm in length and 50 mm in height, with cylinders placed at the entrances of 16.5, 33, 49.5, and 66 mm, respectively. Incompressible, single-phase, laminar، steady-state conditions characterize the fluid flow. The fluid movement inside the computational area was determined by applying finite-volume CFD. The flow distribution was solved using the Navier-Stokes, energy, and continuity equations. The meshing was focused on the equilateral triangular cylinder to ensure that the temperature, pressure, and velocity distribution would be predicted. In this case, the mesh creation for the domain is shown in Figure (2). After analyzing every outcome, recommendations and conclusions were put in writing.

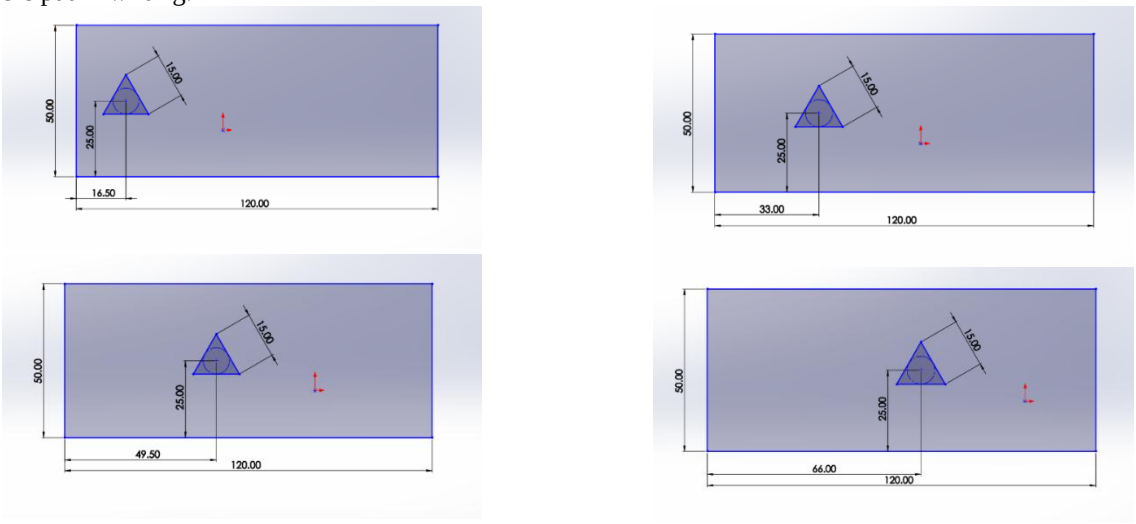

Figure 1. Different positions of an equilateral triangle towards the flow axis inside the computational domain.

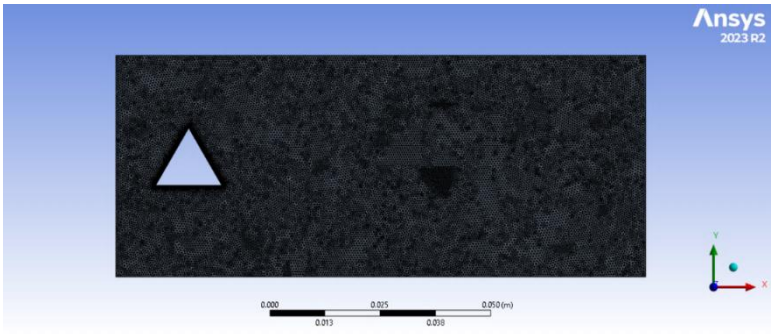

Figure 2. creation mesh of the physical model.

3.2 Mesh Test and Grid Independence

Using successively smaller cell sizes for calculations to set optimization results is what is known as grid independence. When the network becomes small, the calculation must reach the correct result, after which the term is known as network independence. Starting from a rough grid and gradually developing it so that the acquired variables in the values are smaller than the previously determined acceptable error represented by the ordinary CFD technique. The results are tabulated in Table (1) and Figure (3).

Table 1: Result of Mesh Test.

Edge Sizing Number of Divisions	Mesh Elements	Mesh Nodes	Average Outlet Velocity (m/s)
100	51488	26525	0.19201866
150	53777	27898	0.19003168
200	55921	29190	0.18649028
250	57746	30336	0.18628548
300	60170	31775	0.19200026
350	62220	33020	0.18809245
400	65018	34638	0.19307396
450	66305	35491	0.18705967
500	68154	36663	0.19387813
550	70288	37959	0.18708231

600	72386	39230	0.18917826
650	74130	40327	0.18785033
700	76801	41876	0.18705901
750	78684	43034	0.18935041
800	80603	44208	0.19003767
950	87296	48187	0.19055781

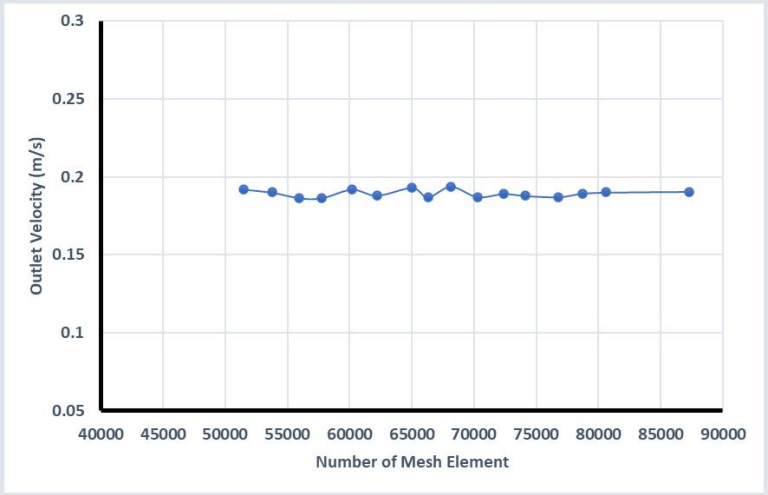

Figure 3. Average outlet velocity of air against many elements meshes.

3.3 Boundary Conditions

The air flow over a cylinder with an equilateral triangular cross-section and an entry temperature of (300 K). For comparison, uniform velocity profiles at the entry and pressure outlet conditions at the outlet zones were used in both air and CFD simulations. The exposed heat flux of (10000 W/m^2) on the cylinder surface is shown in Figure (4). The domain's top and lower walls are considered to be adiabatically insulated, and each iteration step's input data for Re was changed between 100 and 500.

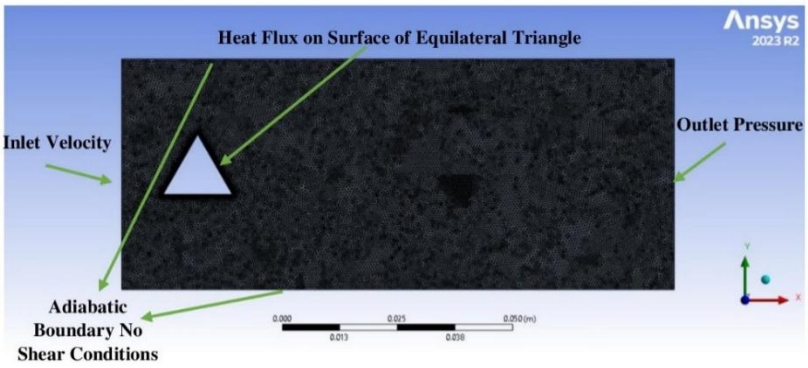

Figure 4. All boundary conditions of the schematic computational domain.

3.4 Solution Technique and Governing Equations

The following are the governing equations for the steady-state incompressible viscous flow [16 and 17]:
Mass conservation (continuity) [16]:

$$\frac{\partial u}{\partial x}+\frac{\partial u}{\partial y}=0 \qquad (1)$$

Momentum conservation in x flow- direction [16]:

$$\frac{\partial u}{\partial t}+u\frac{\partial u}{\partial x}+v\frac{\partial u}{\partial y}=-\frac{1}{\rho}\frac{\partial p}{\partial x}+v\left(\frac{\partial^2 u}{\partial x^2}+\frac{\partial^2 u}{\partial y^2}\right) \qquad (2)$$

Momentum conservation in y flow- direction [17]:

$$\frac{\partial v}{\partial t}+u\frac{\partial v}{\partial x}+v\frac{\partial v}{\partial y}=-\frac{1}{\rho}\frac{\partial p}{\partial y}+\nu(\frac{\partial^2 v}{\partial x^2}+\frac{\partial^2 v}{\partial y^2}) \quad (3)$$

Energy conservation [17]:

$$\frac{\partial T}{\partial t}+u\frac{\partial T}{\partial x}+v\frac{\partial T}{\partial y}=\alpha(\frac{\partial^2 T}{\partial x^2}+\frac{\partial^2 T}{\partial y^2}) \quad (4)$$

Where u and v are the x and y directions of the fluid velocity components (m/s), respectively; p and T are pressure (N/m^2) and temperature of the fluid (K), respectively; ρ, α, and υ are the density (kg/m^3), thermal diffusivity (m^2/s), and kinematic viscosity (m^2/s), respectively. The uniform fluid flow in the x-direction ($u = U_\infty$, $v = 0$) and uniform fluid temperature ($T = T_\infty = 300$ K) are applied at the inlet. The generated buoyancy force in the current investigation is minimal because of the modest temperature difference between T_s and T_∞. Consequently, it seems sensible to limit the analysis of the current formulation to forced convection alone. Furthermore, the flowing fluid's thermophysical characteristics are taken to be temperature-independent. Since it is assumed that the flow is incompressible at low velocities, the influence of viscous dissipation is ignored in the energy calculation. Both the top and bottom boundaries apply the slip flow boundary condition. The outlet specifies the outflow boundary condition.

3.5 Qualities of Convergence

Figure (3) shows the convergence to repeat the solution of the fluid flow equations by stratified flow, and this is what the CFD technique requires, in addition to showing the convergence history of the momentum, continuity, and energy equations. When the solution reaches the accuracy of the numerical convergence criteria, the iterations are stopped using the error residue method. Also, when the residue reaches below the tolerance limit (10^{-6}), the solution is said to converge.

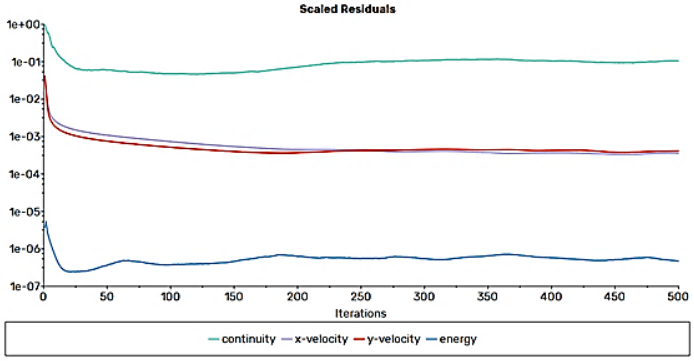

Figure 5. Numerical simulation calculation of history iterations.

4. RESULT AND DISCUSSION

4.1 Dispersal of Temperatures

Figures (6-8) show the temperature distribution on the surface of the cylinder within the computational domain exposed to a constant thermal flux. The location of the cylinder can be observed to affect the change in the temperature distribution of the fluid during the flow within the domain, and also, by increasing the Reynolds number, the surface gain of heat decreases as a result of the high velocity of the air.

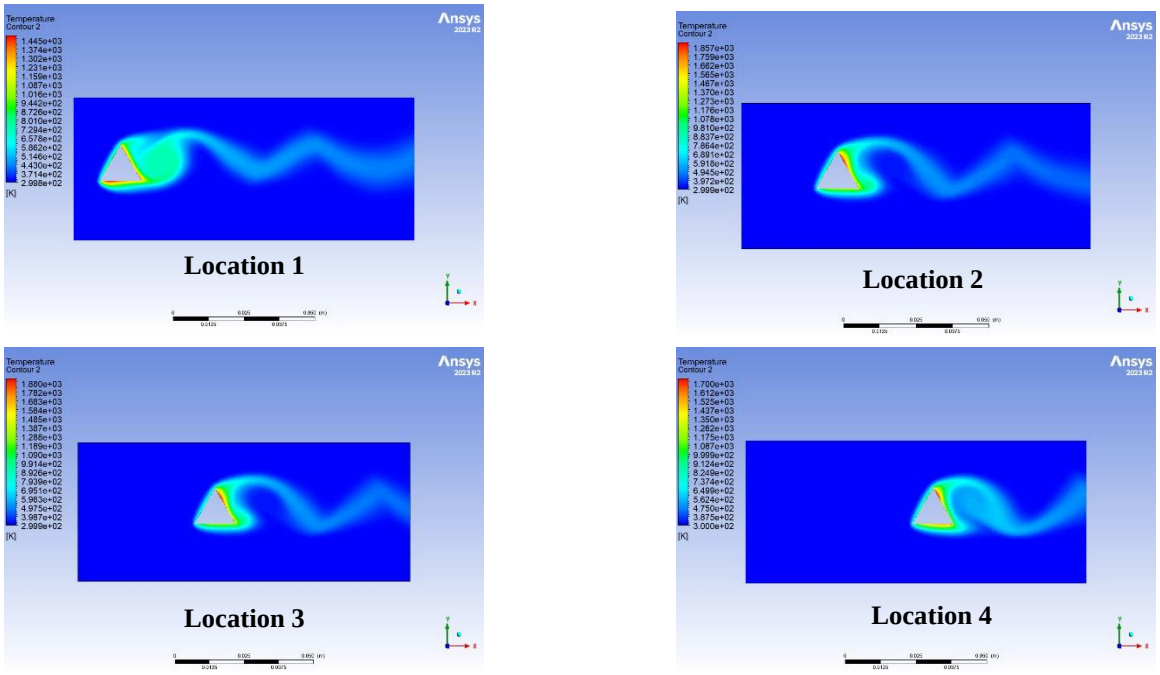

Figure 6: Contour temperatures of various locations for equilateral triangle cylinder at (Re=100).

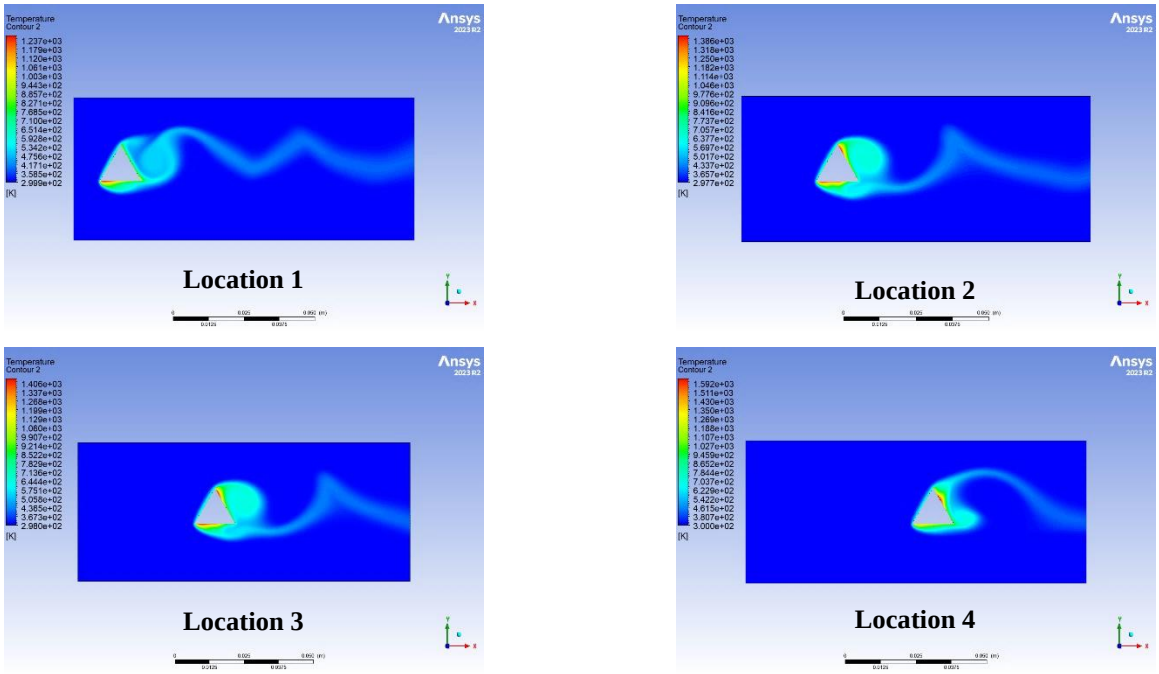

Figure 7.Contour temperatures of various locations for equilateral triangle cylinder at (Re=200).

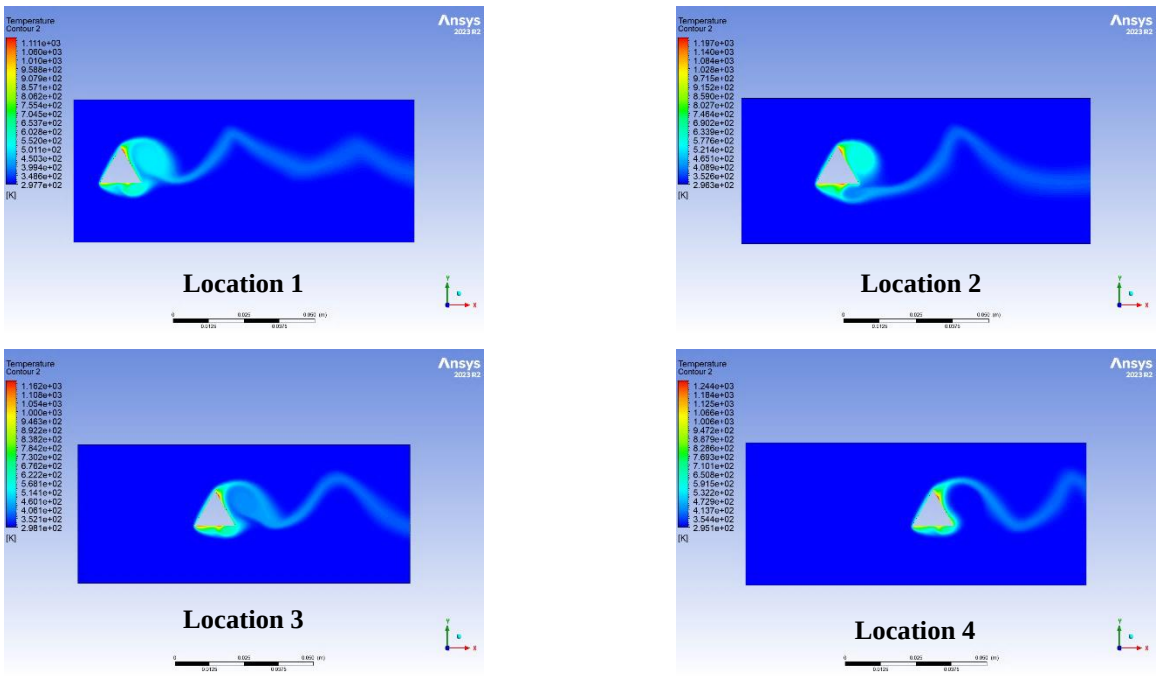

Figure 8. Contour temperatures of various locations for equilateral triangle cylinder at (Re=300).

4.2 Dispersal of Pressure

Figures (9 -11) show the pressure distribution on the surface of the triangular cylinder within the computational domain exposed to a constant heat flux. The location of the cylinder can be observed to affect the change in the distribution of pressure values of the fluid during the flow within the domain, and also by increasing the Reynolds number, the pressure increases as a result of the high velocity of the air. In addition, it can be noted that as a result of the sharp angles of the Triangle, the pressure values are high at the front of the fluid flow compared to other areas.

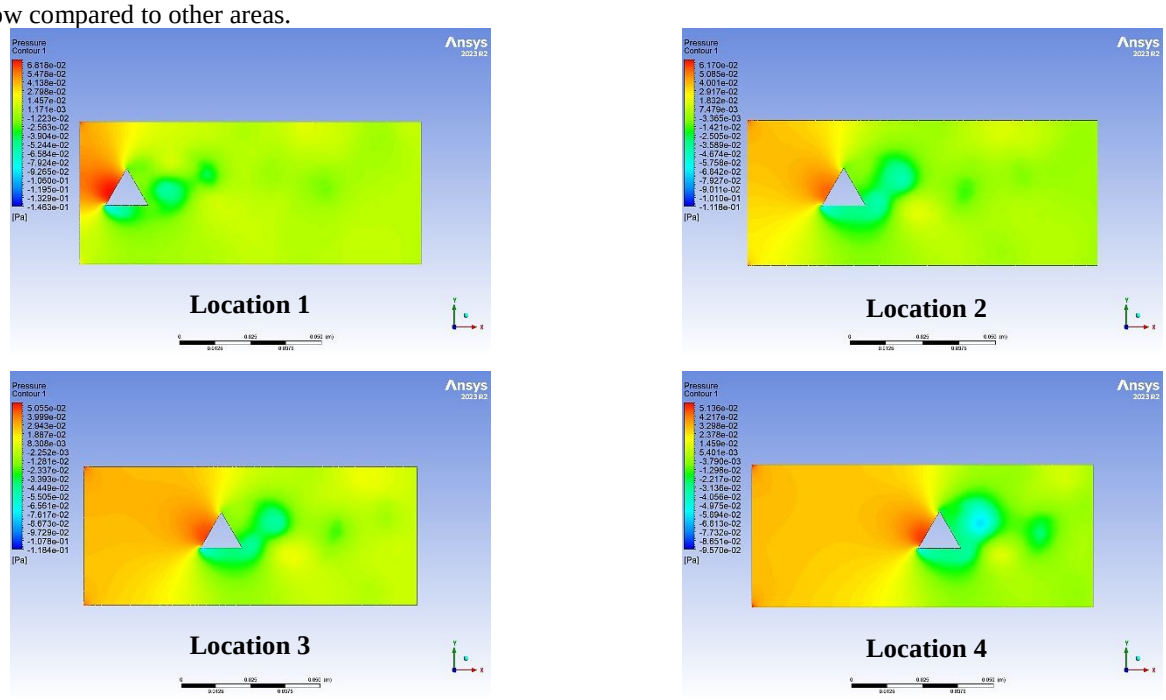

Figure 9 .Contour pressure of various locations for equilateral triangle cylinder at (Re=100).

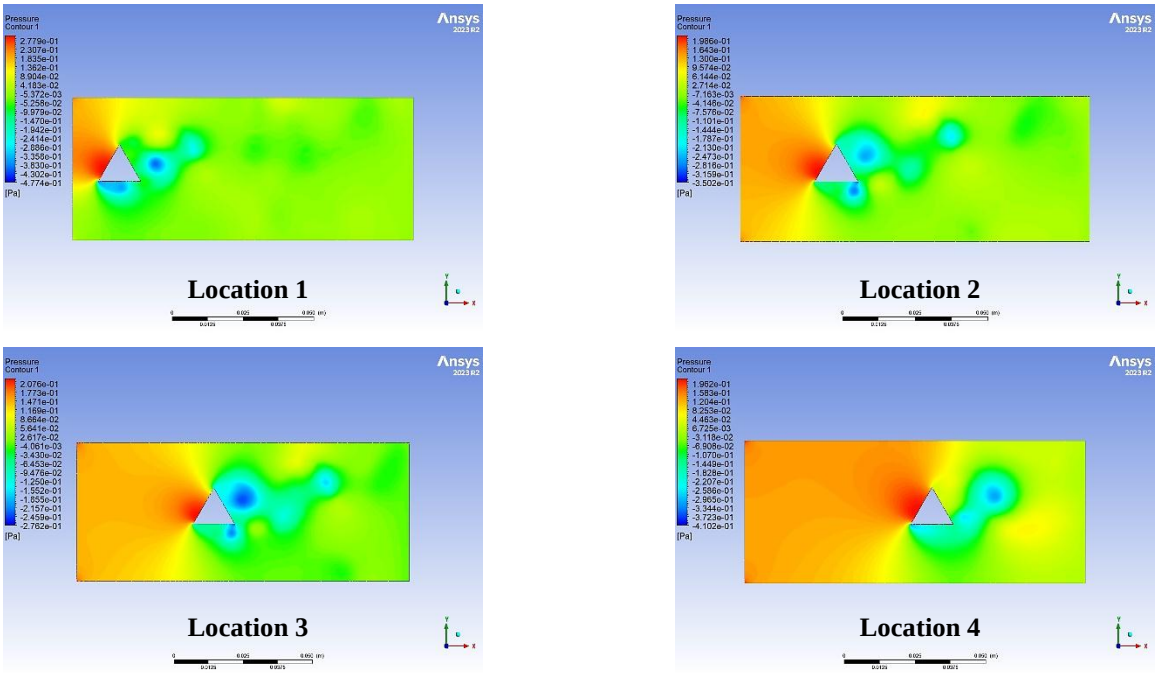

Figure 10. Contour pressure of various locations for equilateral triangle cylinder at (Re=200).

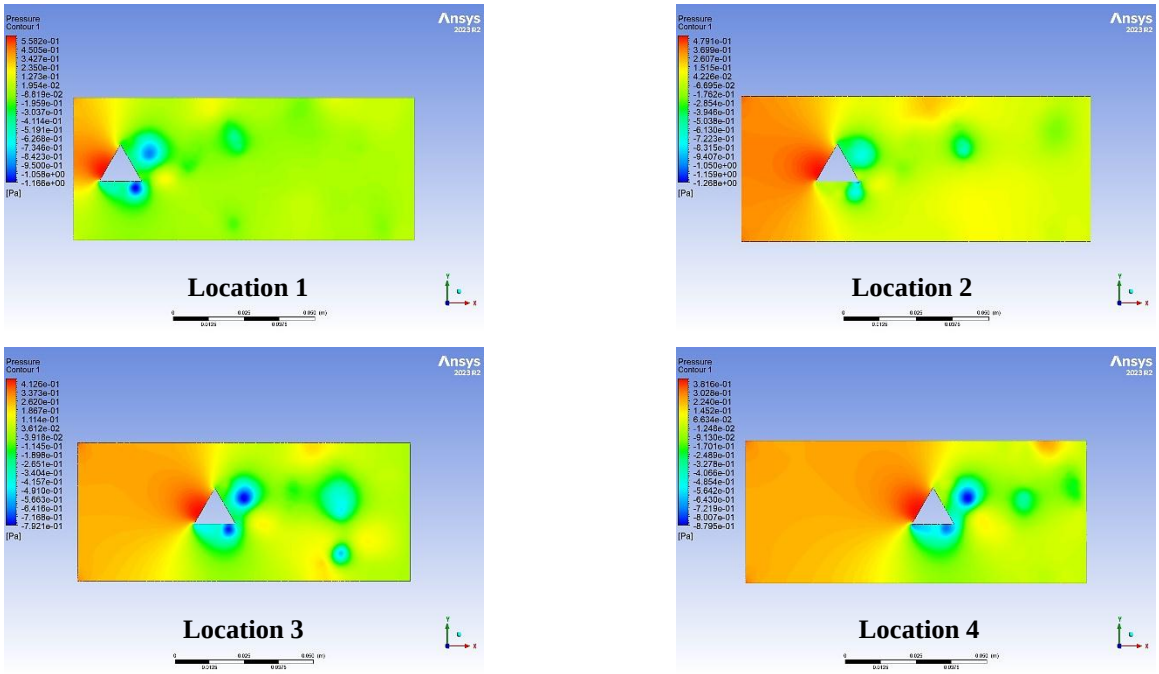

Figure 11. Contour pressure of various locations for equilateral triangle cylinder at (Re=300).

4.3 Dispersal of Velocity

Figure (12-14) indicates fluid velocity distribution around the cylinder at different ranges. The position of the cylinder can be observed to be affected by changing the velocity distribution around the cylinder surface and the computational domain. The velocity distribution decreased by moving the cylinder location away from the fluid inlet, with minimal air velocity observed at the cylinder wall as a result of the boundary layer being in contact with a static object exposed to airflow.

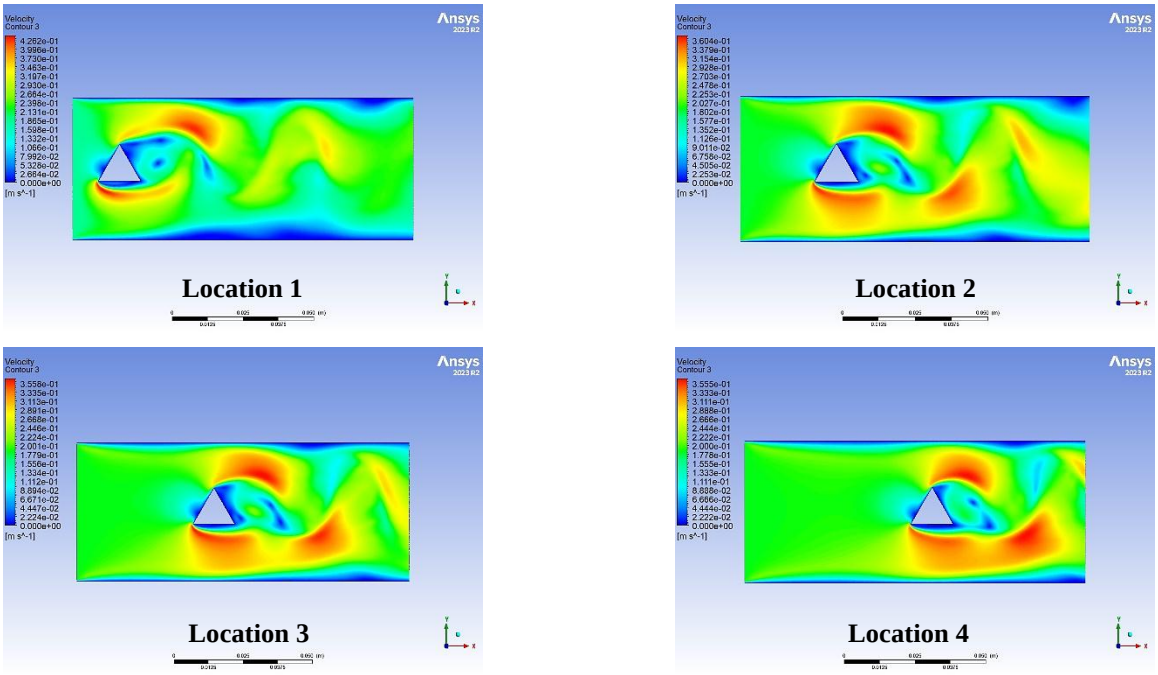

Figure 12. Velocity Contour of various locations for equilateral triangle cylinder at (Re=100).

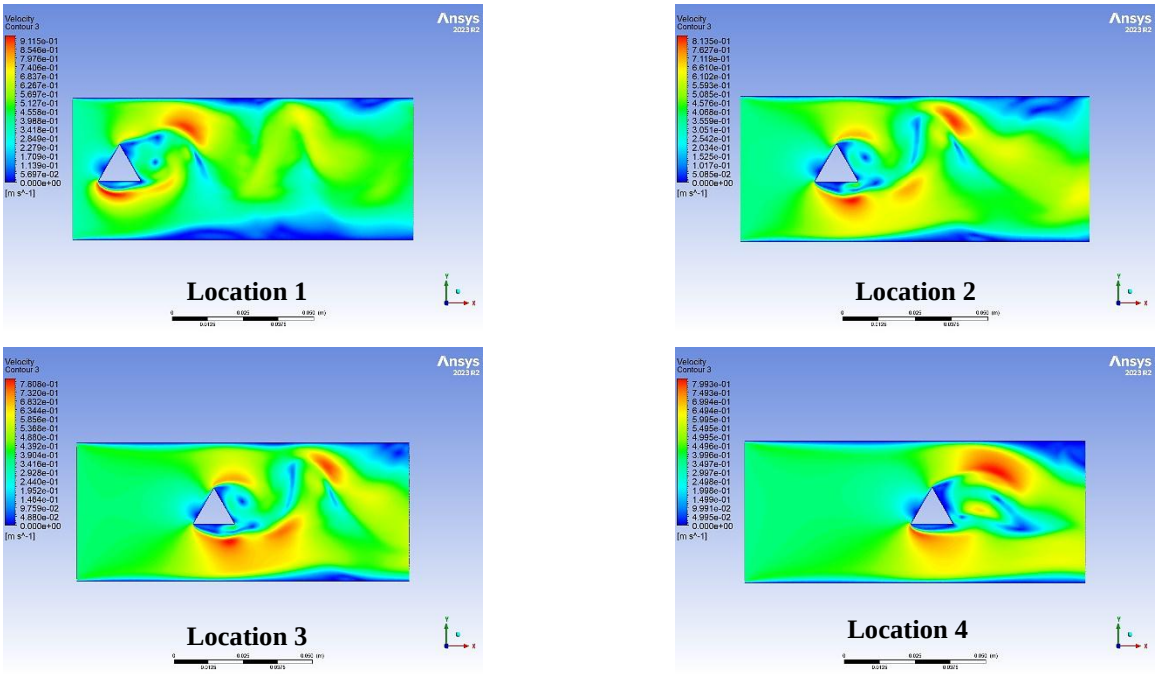

Figure 13. Velocity Contour of various locations for equilateral triangle cylinder at (Re=200).

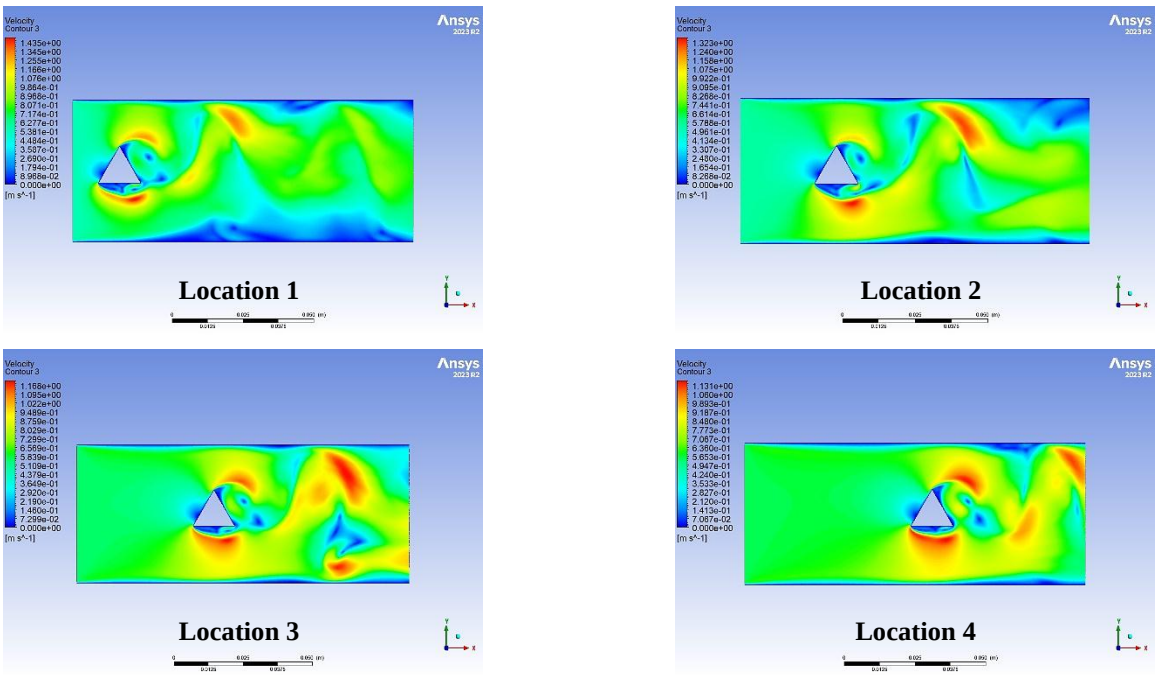

Figure 14. Velocity Contour of various locations for equilateral triangle cylinder at (Re=200).

4.4 Dispersal of Streamline

Figure (15) reveals the fluid flow lines around the cylinder at different extents. The position of the cylinder can be observed to be affected by the appearance of air vortices around the cylinder surface and the computing field. Vortices decrease as the location of the cylinder moves away from the fluid inlet and increase with an increase in the Reynolds number due to an increase in the fluid velocity as a proportional function. The sharp angle of the cylinder's cross-section plays an important role in generating vortices for flow.

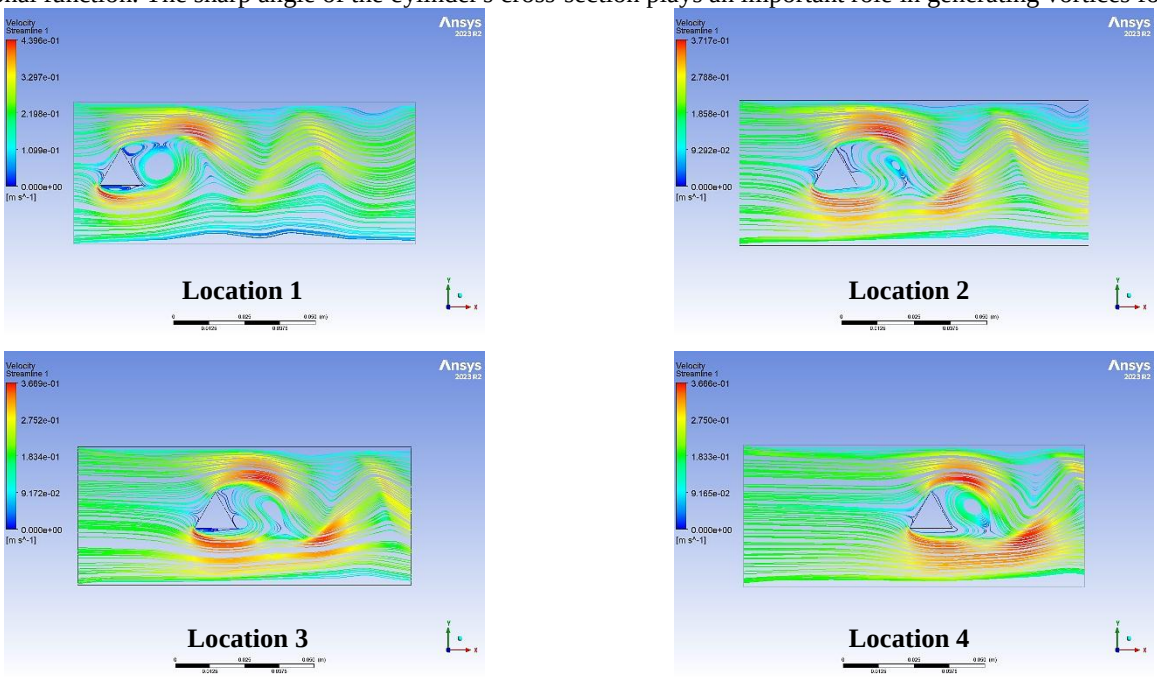

Figure 15. Streamline velocity of various locations for equilateral triangle cylinder at (Re=300).

4.5 Drag and Lift coefficient

Figure (16) shows the change of the drag and lift coefficients against the Reynolds number for different cylinder positions. The highest value of the drag coefficient and lift can be observed in the second location of the cylinder compared to other locations, this indicates that the second location causes an increase in flow obstruction, while the fourth location is ideal because it gives a low drag coefficient.

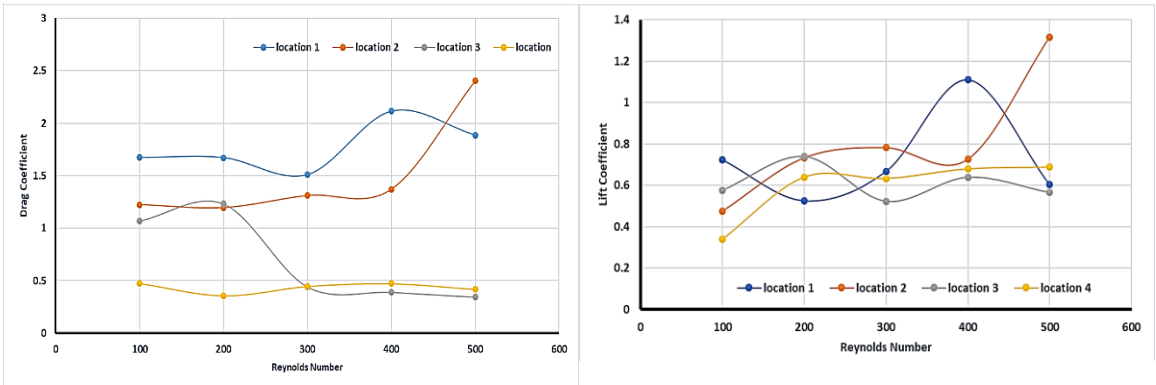

Figure 16. Variation of drag and lift coefficient with Re at different locations of a cylinder.

4.6 Nusselt Number and Surface Temperature

Figure (17) demonstrates the change of the Nusselt number and average temperature of the surface of the cylinder exposed to thermal heat flux against the Reynolds number for different ranges and with a change of the positions of the triangular cylinder. It can be observed that the Nusselt number increases gradually by increasing the Reynolds number due to increasing the coefficient of heat transfer by forced convection, which is a centrifugal function. Also, the first location showed the best improvement in heat transfer compared to the movement of the cylinder towards the airflow. Surface temperatures can be observed gradually decreasing by increasing the Reynolds number as a result of increasing the speed of airflow passing through the computational domain as it is a direct function also when moving away by changing the first location from the other locations, the temperature distribution increases, the last location gave the best heat distribution compared to the other three locations.

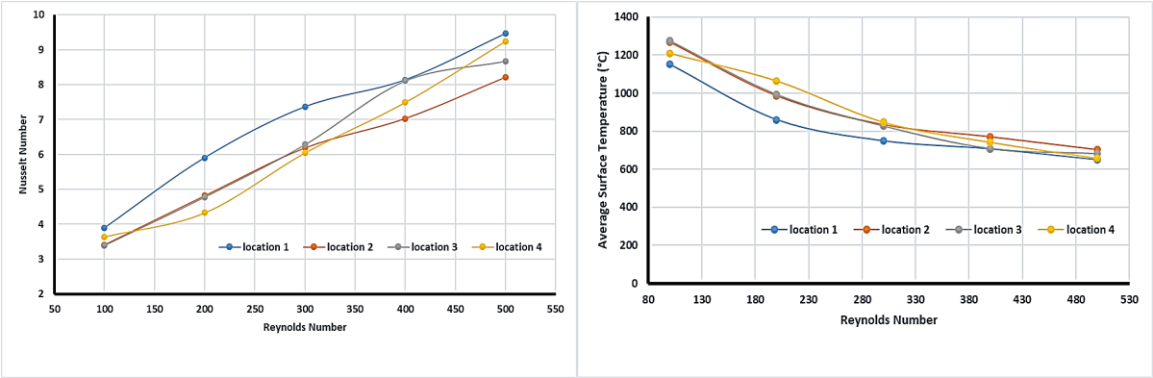

Figure 17. Variation of Nu and average surface temperature with Re at different cylinder locations.

4.7 Friction Factor

Figure (18) displays the change of the friction factor against the Reynolds number at different ranges and for different positions of the triangular cylinder. The friction factor can be observed gradually decreasing by increasing the Reynolds number as a result of increasing the speed of air passing around the cylinder, being an inverse function with the Reynolds number plus the location of the cylinder significantly affecting the change in the amount of the friction factor.

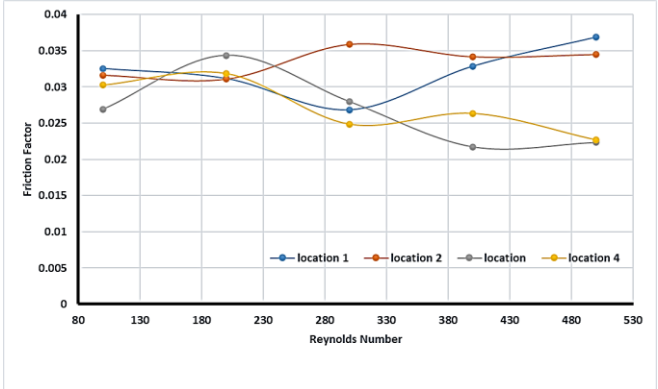

Figure 18. Variation of friction factor with Re at different locations of a cylinder.

5. CONCLUSIONS

In a numerical study using a commercial code (ANSYS Fluent 23.0) to investigate the properties of airflow around a cylinder by changing positions within a computational domain with a single-phase, incompressible, laminar flow in a steady state, the results of the physical phenomenon recorded several signs, as follows:

1- The surface temperature of the cylinder gradually decreases by increasing the Reynolds number and increases by changing the location towards the airflow.
2- The temperature distribution of the computational domain increases as the position of the cylinder changes and decreases with increasing Reynolds number.
3- The pressure distribution of the cylinder within the computational domain decreases as the position of the cylinder changes towards the airflow and decreases with increasing Reynolds number.
4- The velocity distribution of the air around the cylinder within the computational domain decreases as the cylinder position changes towards the flow and increases with increasing Reynolds number due to the proportional relationship.
5- Vortices are generated around the triangular cylinder; the position of the cylinder changes less in the direction of flow and increases with increasing Reynolds number as a result of increasing fluid velocity.
6- The friction factor gradually decreases as the air velocity around the cylinder increases for different Reynolds number ranges.
7- The generation of air vortices behind the triangular cylinder increases by increasing the fluid's velocity due to sharp angles.
8- The temperature distribution rate at the surface of the computational domain at the cylinder positions (2, 3, and 4) differs by a percentage from the first location (48.00, 49.00, and 46.00%), respectively.

ACKNOWLEDGMENT

The author acknowledges the gratitude and appreciation to the Department of Automotive Engineering at the University of Babylon for their support.

List of Symbols

C_D	Drag coefficient (--)
C_L	Lift coefficient (--)
L	Length of the computational domain (mm)
Nu	Nusselt number (--)
P	Pressure of fluid (N/m^2)
Pr	Prandtl Number (--)
Re	Reynolds number (--)
T	Fluid Temperature (K)
T_∞	Temperature free stream (K)
u	velocity in x-direction (m/s)
U_∞	Velocity free stream (m/s)
v	velocity in y- y-direction (m/s)
W	Width of the computational domain (mm)
μ	Dynamic viscosity of working fluid (Pa. s)
α	Thermal diffusivity (m^2/s)
ρ	density of working fluid (kg/m^3)
υ	Kinematic viscosity (m^2/s)

REFERENCES

[1] Boulahia, Zoubair, Abderrahim Wakif, and Rachid Sehaqui. "Heat transfer and cu-water nanofluid flow in a ventilated cavity having central cooling cylinder and heated from the below considering three different outlet port locations." *Frontiers in heat and mass transfer (FHMT)*, vol.11, PP. 1-10, 2018. https://doi.org/10.5098/hmt.11.11

[2] Ranjan, Ram, Amaresh Dalal, and G. Biswas. "A numerical study of fluid flow and heat transfer around a square cylinder at incidence using unstructured grids." *Numerical Heat Transfer, Part A: Applications*, vol. 54, no. 9, pp. 890-913, 2008. https://doi.org/10.1080/10407780802424361

[3] Szczepanik, K., A. Ooi, L. Aye, and Gary Rosengarten. "A numerical study of heat transfer from a cylinder in cross flow." *In 15th Australasian Fluid Mechanics Conference*, pp. 13-17, 2004.

[4] Nasiri, Hossein, Mohammad Yaghoub Abdollahzadeh Jamalabadi, Reza Sadeghi, Mohammad Reza Safaei, Truong Khang Nguyen, and Mostafa Safdari Shadloo. "A smoothed particle hydrodynamics approach for numerical simulation of nano-fluid flows: application to forced convection heat transfer over a horizontal cylinder." *Journal of Thermal Analysis and Calorimetry*, vol. 135 , pp.1733-1741, 2019.

[5] Bouslimi, Jamel, M. A. Abdelhafez, A. M. Abd-Alla, Sayed M. Abo-Dahab, and K. H. Mahmoud. "MHD mixed convection nanofluid flow over convectively heated nonlinear due to an extending surface with Soret effect." *Complexity 2021*, no. 1, 2021. https://doi.org/10.1155/2021/5592024
[6] Sadegh Valipour, Mohammad, Saman Rashidi, and Reza Masoodi. "Magnetohydrodynamics flow and heat transfer around a solid cylinder wrapped with a porous ring." *Journal of heat transfer*, vol. 136, no. 6, pp. 062601, 2014. https://doi.org/10.1115/1.4026371
[7] Ma, Hao, and Zhipeng Duan. "Similarities of flow and heat transfer around a circular cylinder." *Symmetry*, vol.12, no. 4, pp.658, 2020. https://doi.org/10.3390/sym12040658
[8] Maghsoudi, Elham, Michael James Martin, and Ram Devireddy. "Momentum and heat transfer in laminar slip flow over a cylinder." *Journal of thermophysics and heat transfer*, vol. 27, no. 4, pp. 607-614, 2013. https://doi.org/10.2514/1.T3997
[9] Vajravelu, K., K. V. Prasad, S. R. Santhi, and V. Umesh. "Fluid flow and heat transfer over a permeable stretching cylinder." *Journal of Applied Fluid Mechanics*, vol. 7, no. 1, pp.111-120, 2014. https://doi.org/10.36884/jafm.7.01.21135
[10] Smaisim, Ghassan, Oula Fatta, Agustin Valera-Medina, Abdul Rageb, and Nicholas Syred. "Investigation of heat transfer and fluid mechanics across a heated rotating circular cylinder in crossflow." *In 54th AIAA Aerospace Sciences Meeting*, p. 0494. 2016. https://doi.org/10.2514/6.2016-0494
[11] Bharti, Ram Prakash, R. P. Chhabra, and V. Eswaran. "A numerical study of the steady forced convection heat transfer from an unconfined circular cylinder." *Heat and mass transfer*, vol. 43, pp. 639-648, 2007.
[12] Suvanjan Bhattacharyya, et al. "Numerical simulation of flow and heat transfer around hexagonal cylinder." *International Journal of Heat and Technology*, vol. 35.2, pp.360-363, 2017. https://doi.org/10.18280/ijht.350218
[13] Gurminder Singh and Oluwole Daniel Makinde. "Axisymmetric slip flow on a vertical cylinder with heat transfer." *Sains Malaysiana*, vol. 43.3, pp. 483-489, 2014.
[14] Majeed, Afraz Hussain, Rashid Mahmood, Waqas Sarwar Abbasi, and K. Usman. "Numerical computation of MHD thermal flow of cross model over an elliptic cylinder: reduction of forces via thickness ratio." *Mathematical Problems in Engineering* 2021, no. 1 pp. 255-440, 2021. https://doi.org/10.1155/2021/2550440
[15] Yoon, H. S., J. B. Lee, and H. H. Chun. "A numerical study on the fluid flow and heat transfer around a circular cylinder near a moving wall." *International Journal of Heat and Mass Transfer* 50, no. 17-18, pp. 3507-3520, 2007. https://doi.org/10.1016/j.ijheatmasstransfer.2007.01.012
[16] Sunil Chamoli, Tingting Tang, Peng Yu, and Ruixin Lu. "Effect of shape modification on heat transfer and drag for fluid flow past a cam-shaped cylinder." *International Journal of Heat and Mass Transfer*, vol. 131, pp. 1147-1163, 2019. https://doi.org/10.1016/j.ijheatmasstransfer.2018.11.057
[17] Muhammad Jawad, Ziad Khan, Ebenezer Bonyah, and Rashid Jan. "Analysis of hybrid nanofluid stagnation point flow over a stretching surface with melting heat transfer." *Mathematical Problems in Engineering*, vol. 2022.1, pp. 9469164, 2022. https://doi.org/10.1155/2022/9469164